BARD

FINAL REPORT

PROJECT NO. US-3393-03

Synchrotron CMT-Measured Soil Physical Properties Influenced by Soil Compaction

C.J. Gantzer, S. Assouline, S.H. Anderson

2006

10710 6

BARD Research Grant

Final Scientific Report

Cover Page

BARD Project Number: US-3393-03

Date of Submission of the report: 7 February 2006

Project Title: Synchrotron CMT-Measured Soil Physical Properties Influenced by Soil Compaction

Investigators	Institutions
Principal Investigator (PI): Clark J. Gantzer	University of Missouri-Columbia
Co-Principal Investigator (Co-PI): Shmuel Assouline	A.R.O. Volcani Center, Bet-Dagan
Collaborating Investigators: Stephen H. Anderson	University of Missouri-Columbia

Keywords *not* appearing in the title and in order of importance. Avoid abbreviations.
synchrotron, computed microtomography, soil porosity, hydraulic conductivity, pore connectivity, pore tortuosity, and pore size.

Abbreviations commonly used in the report, in alphabetical order:

CMT - computed microtomography, fitting parameters- α and μ, ψ_L- capillary head corresponding to a very low water content, ψ-matric head, θ_s - saturated volumetric water content, θ_L,- the limit of the domain of interest of the WRC, 3DMA-Three Dimensional Medial Axis.

Budget: IS: $ $30,000 US: $ $30,000 Total: $ $60,000

Don R McKinney

Signature

Dona R. McKinney, Associate Director
Office of Sponsored Program Administration

Clark J. Gantzer

Signature

Principal Investigator

Authorizing Official, Principal Institution

UMC Project ID
C00001037

BARD Project Number: US-3393-03. Synchrotron CMT-Measured Soil Physical Properties Influenced by Soil Compaction

Abstract

Methods to quantify soil conditions of pore connectivity, tortuosity, and size as altered by compaction were done. Air-dry soil cores were scanned at the GeoSoilEnviroCARS sector at the Advanced Photon Source for x-ray computed microtomography of the Argonne facility. Data was collected on the APS bending magnet Sector 13. Soil sample cores 5- by 5-mm were studied. Skeletonization algorithms in the 3DMA-Rock software of Lindquist et al. were used to extract pore structure. We have numerically investigated the spatial distribution for six geometrical characteristics of the pore structure of repacked Hamra soil from three-dimensional synchrotron computed microtomography (CMT) computed tomographic images. We analyzed images representing cores volumes 58.3 mm^3 having average porosities of 0.44, 0.35, and 0.33. Cores were packed with < 2mm and < 0.5mm sieved soil. The core samples were imaged at 9.6-μm resolution. Spatial distributions for pore path length and coordination-number, pore-throat-size and nodal-pore volume were obtained. The spatial distributions were computed using a three-dimensional medial axis (3DMA) analysis of the void space in the image. We used a newly developed aggressive throat computation to find throat and pore partitioning for needed for higher porosity media such as soil. Results show that the coordination number distribution measured from the medial axis were reasonably fit by an exponential relation $P(C)=10^{-C/C_0}$. Data for the characteristic area, were also reasonably well fit by the relation $P(A)=10^{-A/A_0}$. Results indicate that compression preferentially affects the largest pores, reducing them in size. When compaction reduced porosity from 44% to 33%, the average pore volume reduced by 30%, and the average pore-throat area reduced by 26%. Compaction increased the shortest paths interface tortuosity by about 2%. Soil structure alterations induced by compaction using quantitative morphology show that the resolution is sufficient to discriminate soil cores. This study shows that analysis of CMT can provide information to assist in assessment of soil management to ameliorate soil compaction.

Objectives of the original research proposal

This study proposed to use synchrotron x-ray computed microtomography (CMT) for measuring effects of compaction on soil hydraulic properties. We investigated the potential of medial axis analysis of CMT data to detect changes in: pore-size distribution, pore-throat-size distribution, coordination-number distribution, and pore-channel length of macropores (matric head $\psi > -0.1$ m H_2O), mesopores ($-0.10 \geq \psi > -3.5$ m H_2O), and some micropores ($\psi < -3.5$ m H_2O) induced by increasing levels of soil compaction.

The project proposes to bridge gaps in the understanding of the relationship between soil structure and hydraulic properties. Changes in soil structure associated with compaction will be evaluated using CMT methods. These methods will be used to quantify macropore connectivity, tortuosity, volume and surface area and to relate these properties to soil hydraulic conductivity. These properties will be determined in soil cores at varying levels of compaction. Measurements and simulated data will be related to theoretical models to predict soil hydraulic properties important to field conditions. Specific objectives include:

1. Measurement of pore connectivity, tortuosity, and size distribution in soil cores as affected by compaction using CMT methods.
2. Estimation of soil hydraulic properties as affected by compaction using pore size distributions obtained from CMT and traditional methods using theoretical models.
3. Assessment of the relationship between soil compaction levels on soil hydraulic properties using CMT technology.

Relevant data, methodology, results, and discussion.

Cores were prepared from Hamra sandy loam soil (Typic Rhodoxeralfs) and Menfro silt loam (Typic Hapludalfs) was shipped to Missouri and packed to three densities using a purpose-built press.

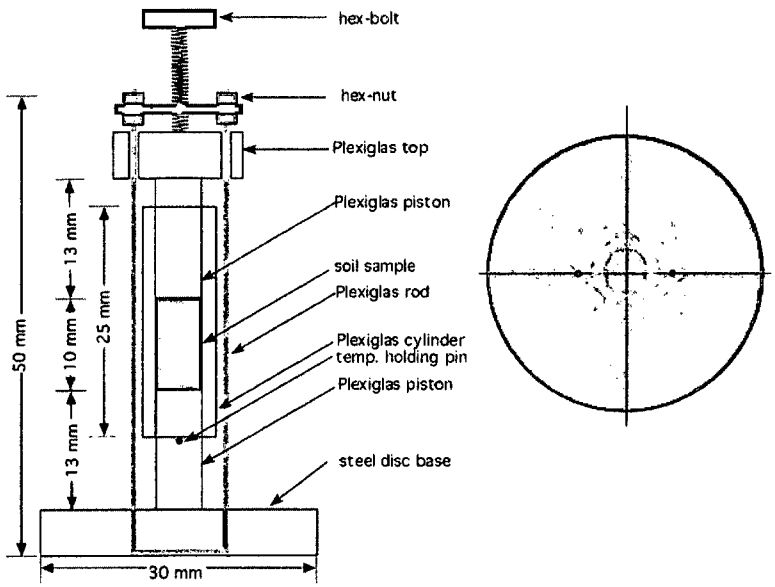

Fig. 1 Press for packing of soil.

The soil densities were 1.50, 1.74, and 1.79 Mg m^3 for the Hamra soil. For reason discussed shortly, the samples from the Menfro while scanned, have not been analyzed because the pore sizes within the aggregates were too small to detect.

X-Ray Computed Microtomography (CMT)

We conducted scanning at the GeoSoilEnviroCARS sector at the Advanced Photon Source (APS) for x-ray computed microtomography (CMT) of the Argonne facility (Rivers, et al., 1999). http://www.techtransfer.anl.gov/techtour/microtomography.html).

We collected absorption CT data on the APS bending magnet Sector 13. The APS bending magnet source has a critical energy of 20 keV, and provides high flux at photon energies up to 100 keV. The beamline provides a 2.5 mrad fan of radiation, with a vertical beam size of about 5 mm. The transmitted x-rays are imaged with a single crystal YAG scintillator, a microscope objective and a 1242x1152 pixel fast CCD detector (Fig. 2). The field of view was set for 5-mm. The system spatial resolution for our work was 9.61 μm.

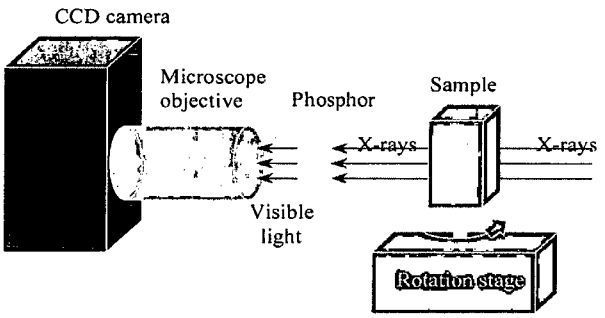

Fig. 2. Schematic of the absorption CT apparatus used on the bending magnet beamline. The configuration is typical of

The GeoSoilEnviroCARS data collection software was be used for initial reconstruction and analysis. This software uses a layered approach. The lowest layer collects a single data frame and allows the user to specify the exposure time, binning factors, region-of-interest and other camera related parameters. The next level is a Visual Basic program, which collects a single CMT data set. This program rotates an object and translates it out of the beam to collect flat field images. Exposure times for a sample are typically 1-3 seconds, with total data collection times in the range of 20 to 40 minutes. The final software layer consists of an IDL (Interactive Data Language) that automates complex experiments. This is often used to collect multiple vertical sections when imaging objects taller than the beam. The system is aligned by imaging a pin that is placed near the edge of the field of view. The pin is imaged at 0, 90, 180 and 270 degree rotations. The data processing consists of 1) preprocessing of image pixels 2) sinogram creation 3) tomographic reconstruction using filtered back-projection. All of the software currently in use at GeoSoilEnviroCARS is written in IDL. The software and documentation is freely available at: http://cars.uchicago.edu/software/tomography.html.

Eighteen (5- by 5-mm) soil sample cores of Hamra sandy loam soil (Typic Rhodoxeralfs) were scanned resulting in a working sample resolution of 350 by 350 by 515 voxels representing a sample volume of 58.3 mm^3. The horizontal scale was set to 1

pixel = 9.61 μm, and the vertical scale was set to 1 slice = 10 μm. Data was also collected for 10- by 10-mm cores, however these cores were beyond the field of view limit of the hardware and could not be scanned properly.

An additional set of cores for the Menfro silt loam (Typic Hapludalfs) was also scanned. However, given the 9.61 μm resolution of scanning the finer interaggregate pores could not be resolved causing an underestimate in the soil total porosity and pore-size.

CMT Image Reconstruction and Analysis

Skeletonization algorithms were used to extract pore structure (Sok et al., 2002). Lindquist and Venkatarangan (1999) and Lindquist et al., (2000) developed a set of algorithms to extract microstructural parameters from CMT 3-D data sets (3DMA, A Package for Geometric Analysis of 2D and 3D Biphase images http://www.ams.sunysb.edu/~lindquis/3dma/3dma.html; Lindquist, 1999). Geometric analysis of a soil core in a gray-scale image required three steps: (1) segmentation, (2) dimensional reduction, and (3) statistical analysis of spatial variation.

Segmentation is the process of converting the gray-scale image into a black and white image by determining an assignment (object or background) for each voxel in the image. The 3DMA provides an algorithm for local thresholding based upon indicator kriging that will be used for the proposed work (Oh and Lindquist, 1999).

Analysis of the geometry of a 3-D object often requires some dimensional reduction. Analysis of the object's geometry is based upon determining and characterizing its 1-D skeleton (or medial axis). The skeleton retains a strict geometric position within the object, and thus preserves much of the fundamental geometry of an object. The 3DMA software also provides for analyses of: (1) distribution of lengths and tortuosities of the shortest connected pathways through the skeleton, (2) position, shape and surface area of the throat (minimum surface area cross section) for each path in the skeleton, (3) distribution of nodal pore volumes (volume associated with each branch cluster) in the skeleton, (4) position, shape and area of grain-grain contact surfaces, and (5) distribution of solid volumes (Lindquist, 1999). We used the medial axis as a tool for the analysis of

geometric structure of void space in soil from CMT data (Lindquist et al, 1996; Lee et al., 1994).

The work of running the computer encountered a number of problems that delayed the calculation of the results until December 2006. The problems dealt with 1) incompatibilities of the computer hardware and software, and 2) the discovery that the 3DMA software had to be rewritten to better assess samples of high porosity using *Aggressive Throat Computation.* This problem will be discusses shortly

Aggressive Throat Computation

Aggressive Throat Computation was used to correct for porous media of-medium/high porosity. In such samples, successful throat finding and pore partitioning is challenging. In analyzing 40-50% porosity samples, the largest pore may account for more than 80% of the entire pore space volume (Prodanovic et al 2005). For this reason, work on the project was delayed because of using the revised software.

Pore Space Analysis

The image analysis algorithms for the pore space consist of six general steps: 1) image segmentation, 2) extraction and modification of the medial axis of the pore space, 3) throat construction using the medial axis as a search path, 4) pore surface construction via marching cubes, 5) assembly of the pore-throat network, and 6) geometrical characterization of the pore-throat network.

Segmentation was done by indicator kriging. Figure3 presents images for the low density Hamra, with Fig. 3c showing the segmented sample and the dark gray color representing the voids.

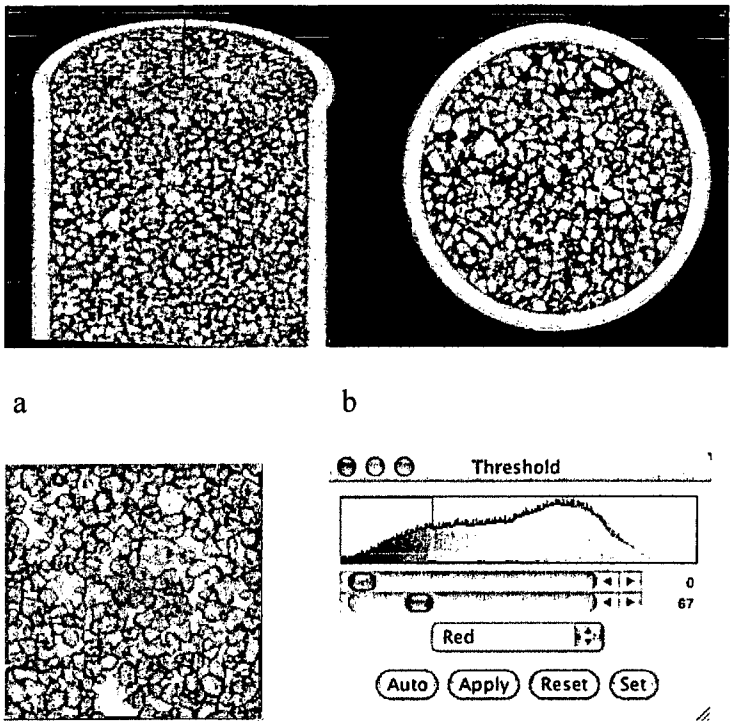

Fig. 3. Tomographic images for the low density Hamra sample. a) 3-d reconstruction, b) one slice from the core, c) segmented image, d) histogram of CT numbers with the red box showing the cutoff value used for segmentation.

Lindquist et al. (2000) developed algorithms to calculate effective pore body and pore throats radii and other geometric properties such as coordination number based on the medial axis of the pore space. The algorithms have been primarily applied to consolidated media, and it is not clear whether they are applicable to higher porosity materials, hence one of the reasons for this study. At larger porosities, standard practice in network flow modeling to regard the void structure in the geological porous media as a network of pore bodies pores with short connections to other of the channels. To analyze a CT image, it is necessary to extract a pore channel network.

Results for traditionally measured and 3DMA estimated porosities versus the bulk densities are presented in Fig 4. Two facts can be observed in this figure. First, there is excellent agreement between the measured and the 3DMA estimated values for the Hamra low and medium densities samples. However, values for the high density is displaced slightly and were too high relative to the measured values. On inspection, it was learned that these samples were compressed so much as to stretch the aluminum cylinder during packing. After correction for stretching, the values show a near 1:1 relationship. Secondly, there is a poor relationship between the measured and the 3DMA estimated values for the Menfro soil. On analysis it was determined that this effect is the result of partial volume rendering of the interaggregate porosity causing failure to detect interaggregate pore space with CMT. Because of this finding, the analysis of the Menfro sample has not be pursued at this time.

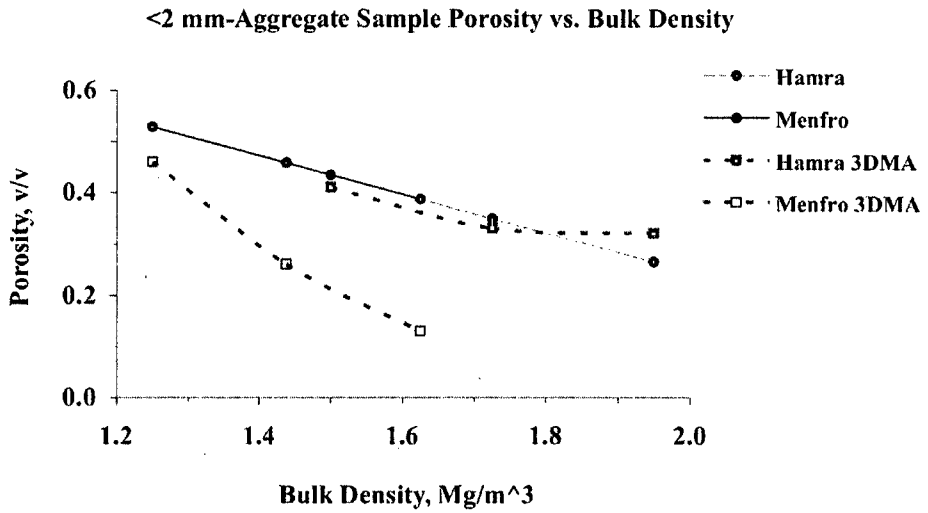

Fig. 4. Porosity vs. bulk density for traditionally measured and the 3DMA estimated values.

Geometric Characterization

As soil properties are statistical, we have characterized the spatial variation of each property by plotting its distribution of values over the image. Distributions are produced for: pore coordination number, pore volume, pore surface area, and throat surface area.

To help with the understanding of the terms Fig. 5 presents a picture of a sample with the medial axis (pore centerline), the pore-throats, and the pores in white, and the solids in gray.

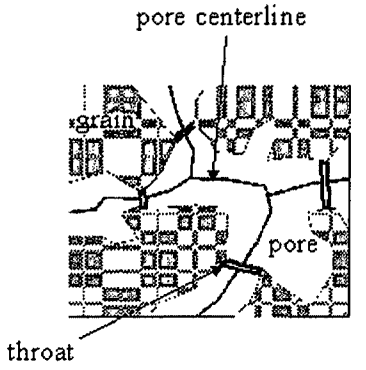

Fig. 5. A picture of a sample with the medial axis colored in red, pore-throats in purple, the pore in white and the solid in gray.

Results presented in Table 1 provide a picture of how pore space changes in Hamra soil as the porosity decreases from increasing compaction. Relatively minor changes in characteristic throat area and average logarithm of nodal pore volume indicate a universality of expansion of channels and nodal pores over all dimensional ranges. The results of the High-density cores compared to the Low-density cores indicate that compression preferentially affects the largest pores, reducing them in size:

porosity decreased by 25% (0.4->0.3)

average pore volume decreased by 30%

average throat area decreased by 26%.

Table 1. Pore characteristics determined from analysis of synchrotron x-ray computer tomography using 3DMA-ROCK medial analysis software.

Hamra Sample	Aggregate Size	Density	Pore Boundry	Pore Internal	Throat Number	NPoreVol Ave	PoreRadius Ave	ThroatArea Ave	ThroatRadii Ave	Coordination 3 Pores
	mm	Mg/m^3	#	#	#	mm^3	micron	micron^2	micron	#
H2L1	<2mm	1.48	1820	4828	29284	0.00129	52.2	4577	33	0.35
H2L2	<2mm	1.48	1810	5336	28686	0.00154	53.2	4638	32	0.37
H2L3	<2mm	1.48	1924	5457	29555	0.00175	55.8	4860	33	0.35
AVE			***1851***	***5207***	***29175***	***0.00153***	***53.7***	***4692***	***32.9***	***0.357***
H2M1	<2mm	1.73	2129	9064	37343	0.00127	51.3	3343	27	0.37
H2M2	<2mm	1.73	2252	9043	35671	0.00131	53.4	3466	28	0.36
H2M3	<2mm	1.73	2325	8316	34048	0.00153	55.8	3914	30	0.34
AVE			***2235***	***8808***	***35687***	***0.00137***	***53.5***	***3574***	***28.5***	***0.356***
H2H1	<2mm	1.77	2129	8489	31374	0.00136	54.5	3582	29	0.40
H2H2	<2mm	1.77	2124	8853	32878	0.00128	53.3	3466	28	0.38
H2H3	<2mm	1.77	2155	9257	34735	0.00122	52.1	3247	27	0.38
AVE			***2136***	***8866***	***32996***	***0.00129***	***53.3***	***3432***	***27.9***	***0.386***
H5L1	<0.5mm	1.48	1696	4213	22711	0.00161	54.7	5252	35	0.38
H5L2	<0.5mm	1.48	1688	4110	24111	0.00101	48.2	4823	33	0.39
H5L3	<0.5mm	1.48	1744	4070	24566	0.00132	51.3	5049	34	0.40
AVE			***1709***	***4131***	***23796***	***0.00132***	***51.4***	***5041***	***33.8***	***0.387***
H5M1	<0.5mm	1.73	2220	9174	36822	0.00130	52.4	3439	28	0.37
H5M2	<0.5mm	1.73	2185	7491	32351	0.00173	56.6	4243	31	0.35
H5M3	<0.5mm	1.73	1871	7985	24953	0.00137	56.6	3920	30	0.39
AVE			***2092***	***8217***	***31375***	***0.00146***	***55.2***	***3867***	***29.7***	***0.370***
H5H1	<0.5mm	1.77	2181	9694	38784	0.00116	50.2	3009	26	0.37
H5H2	<0.5mm	1.77	2250	9584	35777	0.00115	51.0	3042	26	0.38
H5H3	<0.5mm	1.77	2098	8928	34332	0.00127	52.4	3231	27	0.37
AVE			***2176***	***9402***	***36298***	***0.00120***	***51.2***	***3094***	***26.3***	***0.371***

These trends can be clearly seen in Fig. 6.

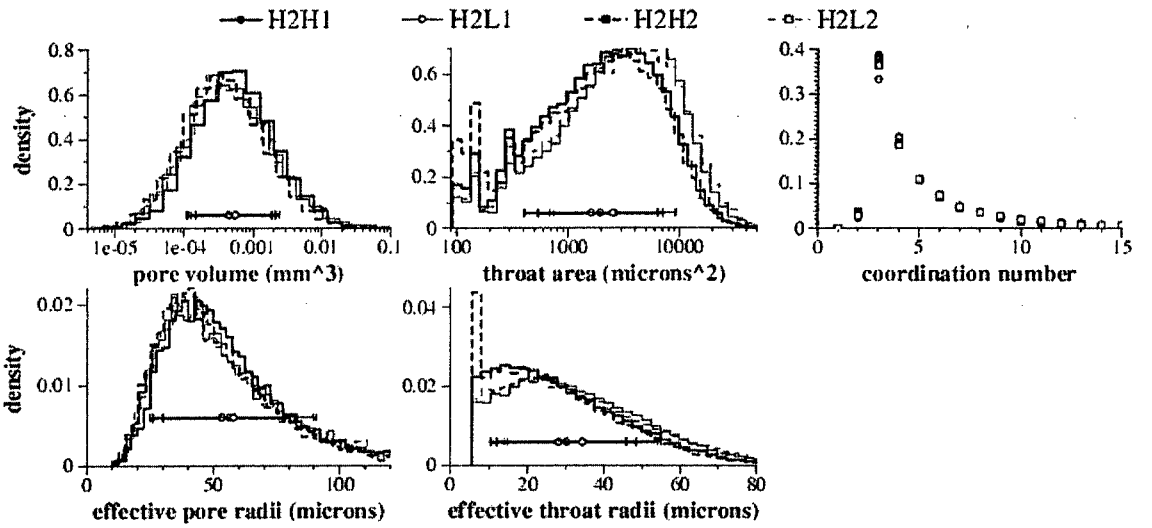

Fig. 6 Comparison of Geometric Characterization for a Low and High density Hamra sample.

Table 2 presents ratios of the averages, showing the amount of change with compaction.

Table 2. Ratios of pore characteristics determined from analysis of synchrotron x-ray computer tomography using 3DMA-ROCK medial analysis software.

Hamra Sample Ratio	Boundry Pore	Internal Pore	Throat Number	NPoreVol Ave	PoreRadius Ave	ThroatArea Ave	ThroatRadii Ave	Coordination 3 Pores
H2L/H2H	0.87	0.59	0.88	1.18	1.01	1.37	1.18	0.93
H5L/H5H	0.79	0.44	0.66	1.10	1.00	1.63	1.28	1.04
H2L/H5L	1.08	1.26	1.23	1.16	1.05	0.93	0.97	0.92
H2M/H5M	1.07	1.07	1.14	0.94	0.97	0.92	0.96	0.96
H2H/H5H	0.98	0.94	0.91	1.08	1.04	1.11	1.06	1.04

There is strong differentiation in the number of interior (non-boundary) pores. Increase in compaction increases the number of pores in the compacted results. Although there are fewer pores in the uncompacted sample, they have larger volumes (or effective radii). The compacted sample High-density cores show a smaller average pore volume than the Low-density samples. There is no consistency in number of throats found, but there are consistent differences in throat area. Higher compaction gives pore-throats of

smaller area (and effective radii). There are also consistent differences in the probability of finding coordination number-3 pores. Higher compaction also gives more coordination number-3 pores. There is little change in coordination number-4 and -5 pores.

To assess the impacts of aggregate size and bulk density, analysis of variance (ANOVA) was conducted on the geometrical data. Results are presented in Table. 3. In no case was it possible to detect differences because of aggregate size. The number of pores and pore-throats and throat size and area are significantly affected by soil compaction. Additionally, there are three slight Aggregate*Density interactions, however they were small compared to the effect of density.

Table 3. Probabilities for pore characteristics determined from analysis of synchrotron x-ray computer tomography using 3DMA-ROCK medial analysis software.

Source	Boundry Pore	Internal Pore	Throat Number	NPoreVo Ave	PoreRadiu Ave	ThroatArea Ave	ThroatRadii Ave	Coordination 3 Pores
Aggregate Size	0.1028	0.1194	0.1353	0.4583	0.3857	0.3994	0.5245	0.0977
Bulk Density	***0.0001***	***0.0001***	***0.0006***	0.2221	0.2294	***0.0001***	***0.0001***	0.128
Aggregate*Density	0.2169	***0.0347***	***0.0409***	0.4048	0.2294	0.0602	0.0566	***0.0298***

Results shown in Fig. 7. indicate that there is a clear separation of the tortuosity of samples between High and Low density samples, with High density (H2H1 - 30% porosity) having greater tortuosity than low compaction (H2L1 - 40% porosity).

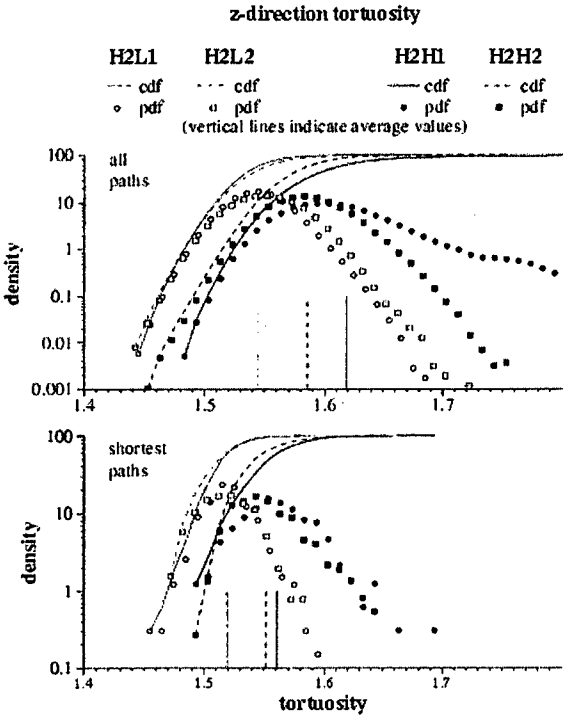

Fig. 7. Comparison of sample tortuosity for Low and High-density Hamra soil cores.

Modeling $K(\theta)$ with Pore Size Distributions

The CMT-measured pore properties and the WRC were to be analyzed using the model of Assouline et al. (1998; 2000). We have not completed the analysis of x-ray CT data with respect to hydraulic flow at this date. The following is the outline we plan to use for this work.

We plan to use the fitted equation:

$$\theta(\psi) = (\theta_s - \theta_L)\{(1-\exp[-(\alpha(|\psi|^{l} - |\psi_L|^{l}))^{\mu}]\} + \theta_L \quad ; \quad 0 \le |\psi| \le |\psi_L| \qquad [1]$$

where α and μ are two fitting parameters, θ_s is the saturated volumetric water content, and ψ_L is the capillary head corresponding to a very low water content, θ_L, representing the limit of the domain of interest of the WRC. In this study, $|\psi_L|$=15 bar, to the 3DMA measured values. Figure 8 presents the measured water release curve for the Hamra soil. Figures 9 and 10 presents α and μ fitting parameters for the Hamra soil.

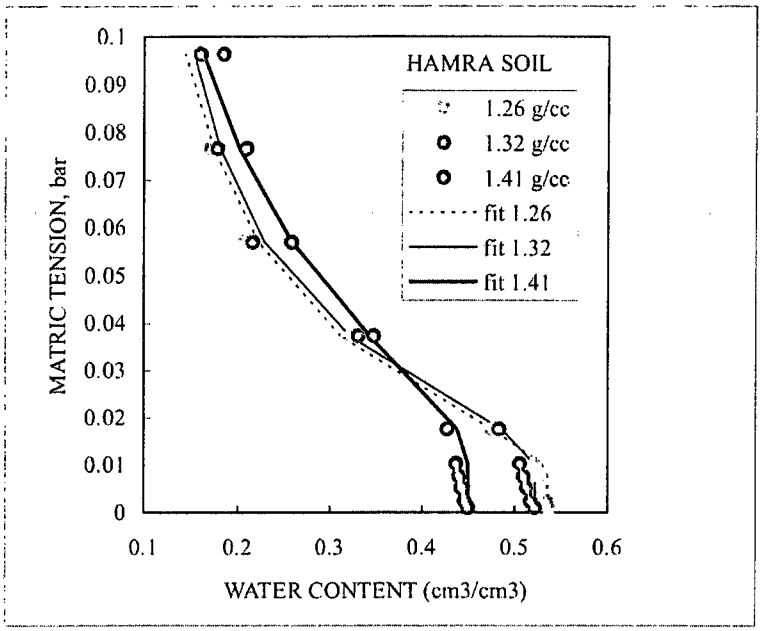

Fig. 8. Soil water characteristic curve for the Hamra soil at low, medium and high bulk densities.

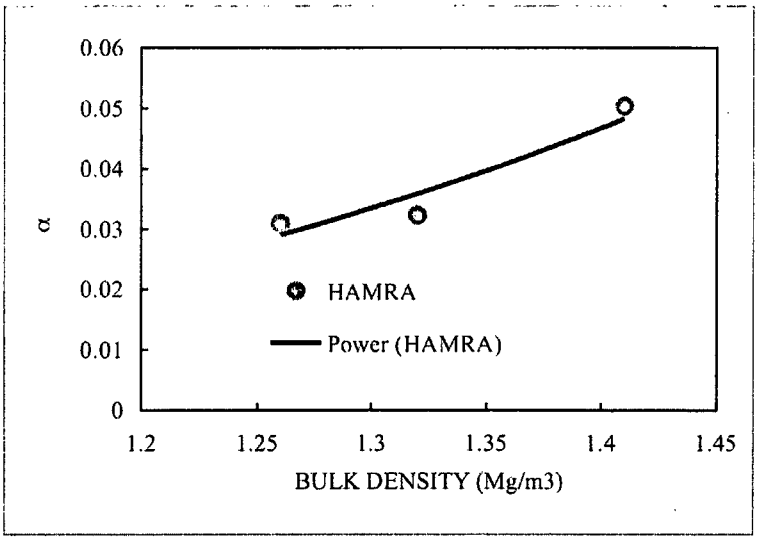

Fig. 9. Soil water fitting parameter α for the Hamra soil at low, medium and high bulk densities.

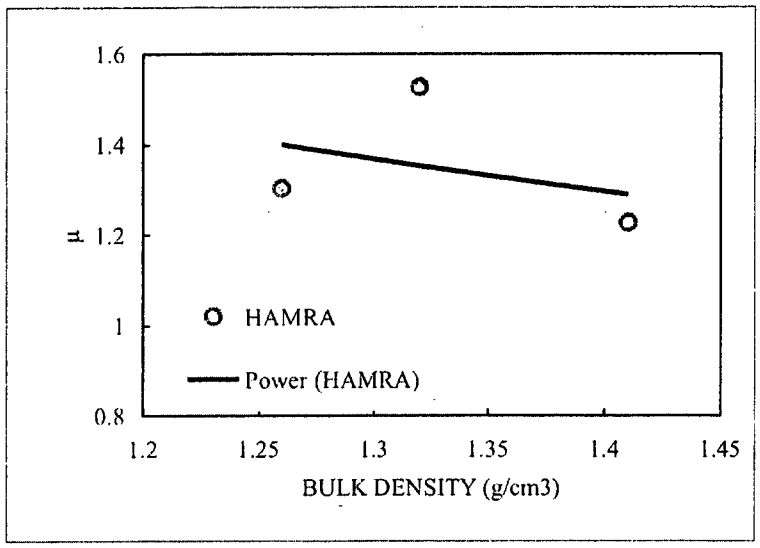

Fig. 9. Soil water fitting parameter μ for the Hamra soil at low, medium and high bulk densities.

The parameter α can be related to the air entry value, meaning some indication on the largest pores in the soil. Therefore, it may be possible to link α and geometrical information from the CMT with the behavior of the large pore under compaction. In addition, μ may be related to the variance of the pore-size distribution and this may lead to some link with geometrical information from the CMT.

We plan to complete this analysis and present the findings at the 18th World Congress of Soil Science July 9-15, 2006 - Philadelphia, Pennsylvania, USA.

Evaluation of the research achievements as relates to the original research proposal and its objectives.

X-Ray Computed Microtomography

Samples of the Hamra and Menfro soil were successfully scanned at the GeoSoilEnviroCARS sector at the Advanced Photon Source (APS) for x-ray computed microtomography (CMT).

Pore Space Analysis

Porosity vs. bulk density for traditionally measured and the 3DMA estimated values were completed.

Geometric Characterization

Pore coordination number, pore volume, pore surface area, and throat surface area. Results of the High density cores compared to the Low density cores indicate that compression preferentially affects the largest pores, reducing them in size; porosity decreased by 25% (0.4->0.3), average pore volume decreased by 30%, average throat area decreased by 26%.

Aggressive Throat Computation

Aggressive Throat Computation was used to correct for media of medium/high porosity media. In such samples, successful throat finding and pore partitioning can be especially challenging. In analyzing 40-50% porosity samples, the largest pore may account for more than 80% of the entire pore space volume (Prodanovic et al 2005). For this reason, work on the project was delayed because of using the revised software.

Modeling $K(\theta)$ with Pore Size Distributions

We plan to complete this analysis and present the findings at the 18th World Congress of Soil Science July 9-15, 2006 - Philadelphia, Pennsylvania, USA.

Description of the cooperation:

List of Presentations:

Gantzer, C.J. S.H. Anderson, and S. Assouline. 2004. Synchrotron Computed Microtomography - Measured Soil Physical Properties Influenced by Compaction. 32nd International Geological Congress. Florence, Italy August 20-28 2004.

Gantzer, C.J. 2005. "Determination of Soil Physical Properties with Computed Tomography." 12 Jan 2005. Dep. of Geological Sciences. Univ. of Texas-Austin.

Gantzer, C.J., S.H. Anderson, and S. Assouline. 2004. Computed microtomography for assessing changes in porosity with compaction. Abst. # 4761. Soil Sci Soc. Am. Annual Meetings, 1-4 Nov 2004 Seattle, WA.

Details of the cooperation:

This project included two researchers from the US and one from Israel. Dr. Gantzer was responsible for the CMT scanning procedures and data analysis. Dr. Anderson assisted in analysis of CMT experiments and analysis of data and the writing of reports. Dr. Assouline worked developing models of soil hydraulic properties as affected by soil compaction. Dr. Assouline also developed procedures for analysis of soil hydraulic properties and modelling of hydraulic conductivity of the soil compaction treatments. The scientific collaboration was based on ideas outlined by the co-investigators. Discussions were carried out mainly by e-mail but also during the mutual visits of the collaborating scientists. Scientific collaboration occurred during the preparation of the annual and final reports and of the joint papers that will result from the project. The final work on this project including modelling of hydraulic conductivity of the soil compaction is expected Summer 2006.

New collaboration also occurred from this BARD grant. A new line of study dealing with characterization and modeling of soil seals using x-ray CT between investigators was initiated. The collection of x-ray CT imagery of the development of soil surface seals related to the duration of rainfall erosivity is ongoing. Data were collected using the high-resolution x-ray computed tomography Facility at the University of Texas at Austin. The purpose of this work is to study the process of soil surface sealing on about 60-soil cores to learn how better to reduce erosion and runoff from intense rainstorms. A second purpose was to facilitate work that will lead to the development of a joint research proposal for submission with Dr. Assouline dealing with this topic. An MS Thesis on this topic will be completed at the University of Missouri during the summer of 2006.

Conclusions:

Compacted soil cores of Hamra and Menfro soil was successfully scanned.

Analysis using 3DMA_rock software package has successfully been done to characterize internal pore geometry.

Data show that parameters determined using 3DMA_rock are able to discriminate difference among cores of different densities.

Due to difficulties, analysis on data from this project is still ongoing. Preliminary results indicate that x-ray CT is capable of extracting meaningful measurements on a 3-D porous body. The success of using this technique to develop estimates of hydraulic properties is yet to be determined. It is expected that analysis of the hydraulic models will be completed by June 2006. Results of this hydraulic modeling will be reported at the 18th World Congress of Soil Science; July 9-15, 2006; Philadelphia, Pennsylvania, USA. These results will be forwarded to the BARD Headquarters.

This study is expected to benefit agriculture by developing tools to nondestructively assess soil structure changes created by compaction, and quantify beneficial effects produced by soil management to manage soil properties damaged by soil compaction. Those who are modeling water movement should expect benefit from soil core analyses by this approach, with improved knowledge of small-scale spatial variability in hydraulic properties.

List of publications

List of Publications: Include only reviewed publications reporting on work at least partially supported by BARD and which includes an acknowledgement to BARD.

None

Report on any patents.

None

Appendix:

References

Al-Raousha, Riyadh, Karsten Thompson and Clinton S. Willson. 2003. Comparison of Network Generation Techniques for Unconsolidated Porous Media. Soil Sci. Soc. Am. J. 67:1687-1700.

Assouline, S. 2002. Modeling soil compaction under uniaxial compression. Soil Sci. Soc. Am. J. 66:1784-1787.

Assouline , S. 2004. Rainfall-Induced Soil Surface Sealing: A critical review of observations, conceptual models, and solutions. Vadose Zone J. 3:570–591.

Assouline, S., D. Tessier and A. Bruand. 1998. A conceptual model of the soil water retention curve. Water Resour. Res. 34: 223-231.

Assouline, S., D. Tessier and A. Bruand. 2000. Correction to "A conceptual model of the soil water retention curve." Water Resour. Res. 36: 3769.

Assouline, S., J. Tavares-Filho and D. Tessier. 1997. Effect of compaction on soil physical and hydraulic properties: Experimental results and modeling. Soil Sci. Soc. Am. J. 61: 390-398.

Ben-Hur, M., M. Agassi, R. Keren, and J. Zhang. 1998. Compaction, aging, and raindrop-impact effects on hydraulic properties of saline and sodic Vertisols. Soil Sci. Soc. Am. J., 62:1377-1383.

Lee, T.C., R.L. Kashyap, and C.N. Chu. 1994. Building skeleton models via 3-D medial surface/axis thinning algorithms. CVGIP: Graph. Models Image Process. 56:462-478.

Lindquist, W.B. 1999. 3DMA General Users Manual. Report No. SUSB-AMS-99-20, Dept. Applied Math. & Stat., SUNY - Stony Brook.

Lindquist, W.B. 1999. 3DMAGeneral Users Manual. [Online]. Available at ftp://ams.sunysb.edu/pub/papers/1999/susb99_20.pdf (verified 3 Feb 2006); Dep. of Applied Mathematics and Statistics, SUNY at Stony Brook, Stony Brook, N.Y. 11794-3600

Lindquist, W.B., S.-M. Lee, W. Oh, A.B. Venkatarangan, H. Shin, M. Prodanovic. 2006. 3DMA-Rock A Software Package for Automated Analysis of Rock Pore Structure in 3-D Computed Microtomography Images. [Online]. Available at

http://www.ams.sunysb.edu/~lindquis/3dma/3dma_rock/3dma_rock.html (verified 3 Feb 2006); Dep. of Applied Mathematics and Statistics, SUNY at Stony Brook, Stony Brook, N.Y. 11794-3600

Lindquist, W.B.; A. Venkatarangan; J. Dunsmuir; and T.F. Wong. 2000. Pore and throat size distributions measured from synchrotron x-ray tomographic images of Fontainebleau sandstones. J. Geophys. Res.-Sol. Earth 105: 21509-21527.

Oh W, Lindquist WB. 1999. Image thresholding by indicator kriging. IEEE Trans Pattern Analysis and Machine Intelligence. 21 (7): 590-602.

Poulsen, T.G., P. Moldrup, B.V. Iversen and O.H. Jacobsen. 2002. Three-region Campbell model for unsaturated hydraulic conductivity in undisturbed soils. Soil Sci. Soc. Am. J. 66:744-752.

Prodanovic

Prodanovic, M., W.B. Lindquist, and R.S. Seright. 2005. Porous structure and fluid partitioning in polyethylene cores from 3D x-ray microtomographic imaging. http://www.ams.sunysb.edu/papers/papers05.html - J Colloid Interface Sci, Elsevier. doi:10.1016/j.jcis.2005.11.053

Rivers, M.L., S. Sutton, and P. Eng. 1999. Geoscience applications of x-ray computed microtomography. Proc. of SPIE, Developments in X-Ray Tomography II, Vol 37(72), 78-86.

Sok R.M., M.A. Knackstedt, A.P. Sheppard, W.V. Pinczewski, W.B. Lindquist, A. Venkatarangan, and L. Paterson. 2002. Direct and stochastic generation of network models from tomographic images; Effect of topology on residual saturations. Transport in Porous Media 46 (2-3): 345-372.

Publication Summary (numbers)

	Joint IS/US authorship	US Authors only	Israeli Authors only	Total
Refereed (published, in press, accepted) BARD support acknowledged				
Submitted, in review, in preparation	1			1
Invited review papers				
Book chapters				
Books				
Master theses	1			1
Ph.D. theses				
Abstracts	4			4
Not refereed (proceedings, reports, etc.)				

Postdoctoral Training: List the names and social security/identity numbers of all postdocs who received more than 50% of their funding by the grant.

Cooperation Summary (numbers)

	From US to Israel	From Israel to US	Together, elsewhere	Total
Short Visits & Meetings	1	1		2
Longer Visits (Sabbaticals)				

Description Cooperation:

Patent Summary (numbers)

	Israeli inventor only	US inventor only	Joint IS/US inventors	Total
Submitted				
Issued (allowed)				
Licensed				